24th COBEM - 2017

24th ABCM International Congress of Mechanical Engineering
December 3-8, 2017, Curitiba, PR, Brazil

COBEM-2017-0920
MECHANICAL ANALYSIS OF THE ADAPTATIVE HIP GUIDE FOR PERIACETABULAR OSTEOTOMY SURGERY

Fabiane Grazielle Silva
Flávia de Souza Bastos
Universidade Federal de Juiz de Fora, Rua José Lourenço Kelmer, S/n - Martelos, Juiz de Fora - MG, 36036-330
fabiane.grazielle@engenharia.ufjf.br
flavia.bastos@ufjf.edu.br

Alexandre da Silva Scari
Universidade Federal de Juiz de For a, Rua José Lourenço Kelmer, S/n - Martelos, Juiz de Fora - MG, 36036-330
alexandre.scari@engenharia.ufjf.br

Bruno Gonçalves Schroder e Souza
Universidade Federal de Juiz de For a, Rua José Lourenço Kelmer, S/n - Martelos, Juiz de Fora - MG, 36036-330
brunogss01@yahoo.com.br

Abstract. *Osteoarthritis is a progressive and irreversible condition, where there is loss of articular cartilage causing pain and in some cases deformity, especially in weight-bearing joints such as the hip joint. From the social and economic point of view the impacts are enormous, since the arthrosis reduces the quality of life of the affected patients and its treatment involves procedures with great cost. In this context, the study of three-dimensional modeling and rapid prototyping procedures are the key to the development of methodologies that help in the prevention and correction of joint disorders. In this work, mechanical analysis of the adaptive hip guide 3D (three-dimensional) printed in ABS polymer for periacetabular osteotomy surgery was developed. Firstly, tensile tests were performed to determine the mechanical properties of the 3D printed ABS polymer. To evaluate the design of the surgical guide, a computational model was made using Meshmixer. To reduce the computational cost, a simplified model of the guide was generated using Abaqus geometric tools. The finite element analysis was performed and the Tresca stress distribution was evaluated for different conditions of surgical procedure. After the analysis it is possible to verify if the surgical guide is effective in its function of assisting in periacetabular osteotomy surgery.*

Keywords: *osteoarthritis, ABS polymer, 3D printing, tensile test, finite element analysis.*

1. INTRODUCTION

Osteoarthritis is a public health problem. It is a degenerative disease of the joints, with a progressive character and multifactorial etiology, which decreases the quality of life and the function of the affected individuals. It is estimated that the prevalence is 22% in the United States population (Bitton, 2009), where more than 253,000 total hip arthroplasty surgeries was performed per year, costing hundreds of millions of US dollars. In Brazil, between January 2013 and October 2015, 36,420 total hip arthroplasties were performed, by the Unified Health System (SUS), with a total cost of 156,039,232.75 reais (Ministry of health - BR, 2016).

For the treatment of the arthrosis, the surgical procedure of periacetabular osteotomy is performed. This procedure is destructive, cutting the pelvis in order to leave the acetabulum free for the correction of the acetabulum-head the femur contact. Surgical chisels penetrate the pelvis in predetermined directions and angles (Ganz et al,1988). Figure 1a shows the surgical planning of the periacetabular osteotomy procedure.

According to Claudio Luís Hayasaki and E. A. Capello Sousa (2006), three-dimensional modeling is a consistent tool for the aid of problem solving in biomechanics. They validate the use of three-dimensional modeling together with the Finite Element Method to evaluate the behavior of the bone structure of the rabbit tibia.

The Finite Element Method has been used to analyze stresses from the surgical procedure of periacetabular osteotomy. Chegini et al. (2009) determined the distribution of tensions to a hip after correction using this same methodology.

The goal of this study is to analyse the mechanical behavior of the 3D-printed surgical guide and determine its design for an efficient assistance the insertion of the surgical chisels in the periacetabular osteotomy surgery. The Figure 1b

shows Conceptual representation of the guide prototype in modeling compound, adapted to a plastic model of the bone, in reduced scale, and markings of planes where penetration of surgical chisels should occur.

Figure 1. (a) Three-dimensional representation of surgical planning of periacetabular osteotomy; (b) Conceptual representation of the guide prototype in modeling compound;

2. MATERIAL AND METHODS

2.1 Computational modeling of guide using Meshmixer

In the environment of computational biomechanics, it is possible from 3D models to generate physical parts using rapid prototyping. In this work, the computational model of the pelvis was built with Meshmixer, which is a free software from Autodesk intended to create 3D objects. It contains different tools that allow the generation from simple geometries to the more complex ones.

For the development of the guide in Meshmixer, the region of interest was first selected using the selection tool, observing the anatomy of the hip bone and the position where the cut chisels should be inserted. Then, the "offset" tool allowed the generation of a negative of the hip bone. The guide was generated with a thickness of 10 mm. The 3D model of the surgical guide in a simple way as shown in Figure 2.

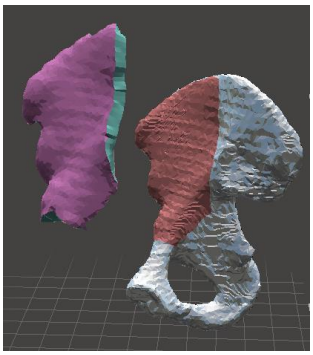

Figure 2. Computational model of surgical guide generated in Meshmixer.

2.2 3D printing protocol

Six specimens were 3D-printed in ABS polymer. Their dimensions are based on Type 1 (see Figure 3) from ASTM 638-02a standard, which presents instructions for tensile tests of polymer specimens. The geometric 3D model of the specimens was built in SketchUp software.

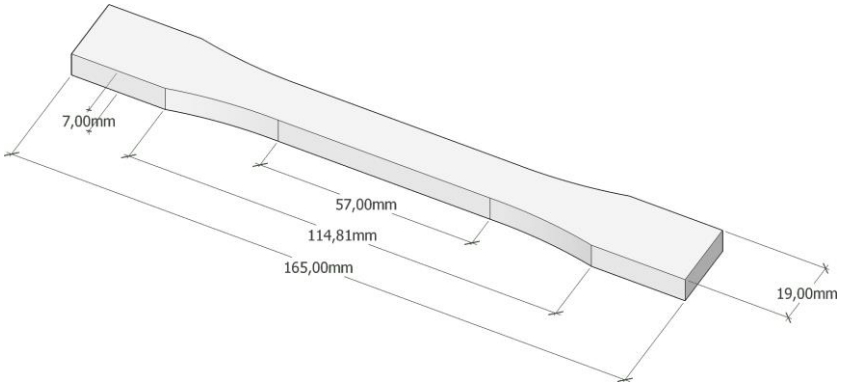

Figure 3. Specimen dimensions according to ASTM 638-02a standard.

The 3D file model (.STL) was imported into Repetier Host (version 2.0.1) and five copies were added in the impression area (see Fig. 4). The six models were positioned within the printing table area. For the slicing the software Slic3r was used, which is part of the Repetier Host software. Figure 6 shows the six models sliced.

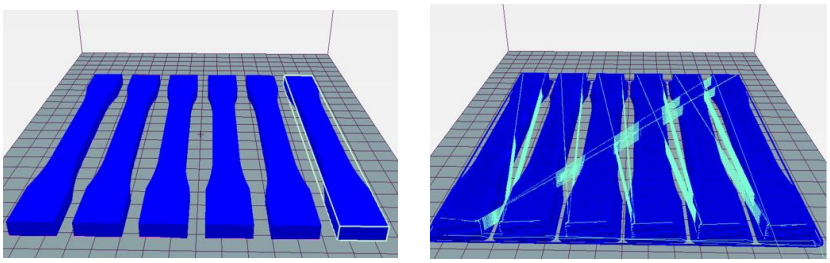

(a) (b)

Figure 4. (a) 3D models of the six specimens; (b) Sliced 3D models in Slic3r software, built in Repetier Host software.

After slicing the models, the printing variables were adjusted (see Tab. 1 and Tab 2). The 3D printings were made at room temperature, with a GTMax3D printer and grey ABS with 1.75 mm diameter. Figure 5 shows the 3D-printed specimens. In order to compare their strength, the 3D printings were done considering two principal directions: 0 degree and 90 degrees.

Table 1. 3D printing protocol for layer thickness and fill settings.

Property	Value	Unit
Layer Heigth	0,2	mm
First layer heigth	0,32	mm
Fill density	100	%
Fill angle	0	degrees

Table 2. Printing protocol for print speeds settings.

Speed for print moves	Value	Unit
Perimeters	40	mm/s
Small perimeters	80	%
External perimeters	40	%
Infill	60	mm/s
Solid infill	60	%
Top solid infill	40	%

Figure 5. 3D-printed specimens in ABS polymer, 0 degrees.

The 3D filament mechanical properties are presented in Table 3.

Table 3. 3D filament mechanical properties. Adapted from Ultimaker (2017).

Mechanical property	Value	Unit
Elastic modulus	1681.5	MPa
Tensile stress at yield	39.0	
Tensile stress at break	33.9	

2.3 Tensile tests

A universal tensile testing machine made by EMIC was used to perform the tests (see Fig. 6), which has a capacity up to 50 kN. After the specimen was fixed in the testing machine, the load cell was connected and the displacement of the clamp was set up in order to cause the failure of the specimen.

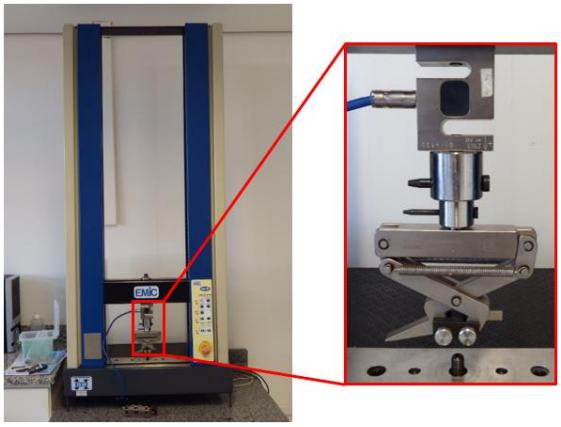

Figure 6. Universal tensile testing machine made by EMIC.

Six specimens 3D-printed at 90 degrees direction were tested and, for comparison, an additional specimen was 3D-printed at 0 degree direction. The tests were performed at a room temperature and, according to standard ASTM 638-02a, for Type 1 specimen the test speed shall be 5 mm/s.

After the tests, with the flange displacements and the respective forces applied for each instant of time, the stress-strain curves can be determined, along with the yield stress, the tensile stress at break and the Young's modulus. The transversal section area of the specimens was 91mm^2.

Mechanical properties such as the yield strength (σ_y) and the Young's modulus (E) was be obtained. The stress (Eq. 1), the strain (Eq. 2) and the Young's modulus (Eq. 3) was be calculated as follows:

$$\sigma_y = \frac{F}{A} \tag{1}$$

Where *F* is the force applied and *A* is the initial cross-sectional area of the specimen.

$$\varepsilon = \frac{L_f - L}{L} \tag{2}$$

Where ε is the strain and L_f and L are the final and initial length of the specimen, respectively.

$$E = \frac{\Delta\sigma}{\Delta\varepsilon} \tag{3}$$

Where $\Delta\sigma$ is the increased stress and the $\Delta\varepsilon$ is the increased strength.

2.4 Simplified Model in Finite Elements

For the finite element analysis, a simple preliminary model of the guide was developed, which contains a flat structure with one cavity to insert the chisel. Figure 7 shows the preliminary model of the guide created in Abaqus with the geometric tools available in the software.

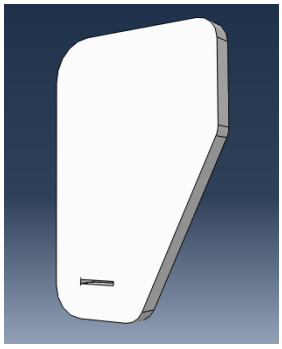

Figure 7. Simplified three-dimensional model of the surgical guide.

To complete the model, two more parts were created. One represents the hip bone and, the other, the cutting chisel. The simulated surgical procedure consisted in pushing the cutting chisel against the bone. What complicates the model is that the hammering that the surgeon imposes on the bone is not centralized. This eccentric hammering may cause the guide to fail. To simulate the actual movements and efforts of periacetabular osteotomy surgery, rotations were imposed on the cutting chisels, simulating the eccentricity of the surgeon's hammer.

A similar geometry to the guide was constructed to represent the hip bone to be operated. Its properties are presented in Table 3. The chisels for hip arthroplasties are usually rectangular, with a constant cross section, and made of martensitic stainless steel. Its properties are also shown in Table 4. The chisel has 150 mm in length, 19 mm in width and 2 mm in thickness. The cutting tip of the chisel has 1 mm in thickness.

Table 4. Properties for hip bone and stainless steel: density, Elastic modulus, Poisson's coefficient. Adapted from Dalstra et al., (1993), AKSteelCorporation (2007) and Callister, (2007).

Part	ρ (kg/mm^3)	E (MPa)	υ
Hip bone	$3{,}54^{-4}$	24500	0,40
Stainless steel	$7{,}74^{-6}$	200000	0,28

The properties of the 3D-printed guide in ABS polymer were calculated with Eq. 1, 2 and 3. For the finite element model, the mean elastic modulus of the six specimens was considered. The value considered for the Poisson's coefficient was 0.37, according to Cantrell et al. (2017).

The guide is secured to the bone by three screws. To simulate the screws, three circumferences with a diameter of 4 mm were constructed on the lower surface of the guide and on the upper surface of the bone. The 'Tie Constrain' tool was used to glue these surfaces that were previously drawn to the bone and to the guide.

The three parts (chisel, hip bone and guide) received tetrahedral mesh elements, with 3438, 21833 and 17648 elements, respectively. The elements were of the type C3D10: a ten-node quadratic tetrahedral. The mesh in the contact regions between the chisel and the guide cavity, between the chisel and the hip bone was refined. Figures 8a, 8b and 8c shows the finite element meshes of the guide, the chisel and hip bone.

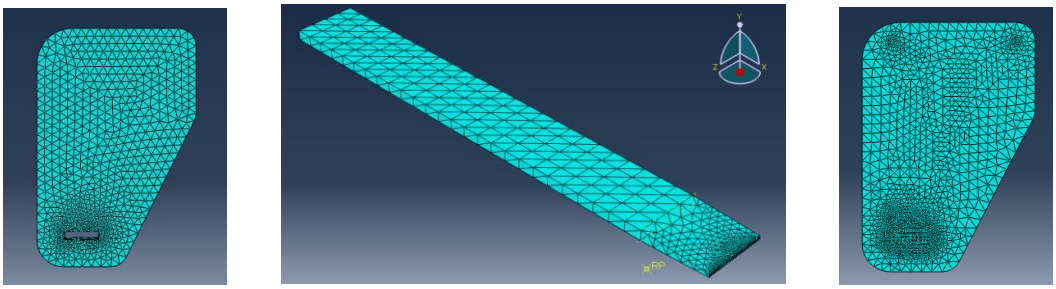

a) Guide mesh b) Chisel mesh c) Hip bone mesh

Figure 8. Finite element mesh with tetrahedral elements and mesh refinement regions.

The finite element analysis performed has two steps. In the first step, the bone was fixed in its borders where all the 6 DoF (degrees of freedom) were restricted. The guide was fastened to the bone by the three screws. For the chisel, only the displacement in the Z-axis was free where a displacement of -10mm was imposed. This movement is done by the surgeon to engage the chisel in the guide before the hammering starts. Then, the second step simulates the chisel displacement and rotation in relation to a reference point in the guide. This movement simulated the eccentric penetration of the chisel in the hip bone.

The contact between the chisel and the guide was defined by 'Frictionless contact', simulating a low coefficient of friction between the chisel and the guide. The contact with normal behavior was set up as 'Hard contact' in order to avoid the penetration of one another. The same conditions are used to define the contact between the chisel and the bone.

By preliminary simulation, it was determined that the displacement in the Z-axis of -10.012 mm leads to a stress of 119 MPa, sufficient to cut a bone. Iplikcioglu and Akca (2002) showed that stresses between 100 MPa and 130 MPa are necessary to fracture the bone. Different rotations were simulated to ascertain the maximum possible rotation angle of the chisel without fracturing the guide.

3. RESULTS

3.1 Experimental tests

Table 5 presents the experimental results summary for each specimen subjected to tensile test and also the calculation results (strain, stress, and Young's modulus).

The Figures 9a and 9b show the failure sections of the specimens printed at 0 degree and 90 degrees.

The stress-strain curves obtained experimentally are presented in Figure 10.

Table 5. Experimental results summary - 3D-printed specimens at 0 degree.

Specimen	Maximum stress (MPa)	Maximum strength	Tensile stress at break (MPa)	Young's modulus (MPa)
1	33,24	0,196	33,24	220,40
2	33,64	0,167	33,62	284,12
3	34,43	0,158	34,40	314,71
4	35,54	0,179	35,48	266,30
5	35,02	0,169	34,94	308,58
6	35,78	0,171	35,72	290,39
Average value	34,60	0,173	34,57	280,75

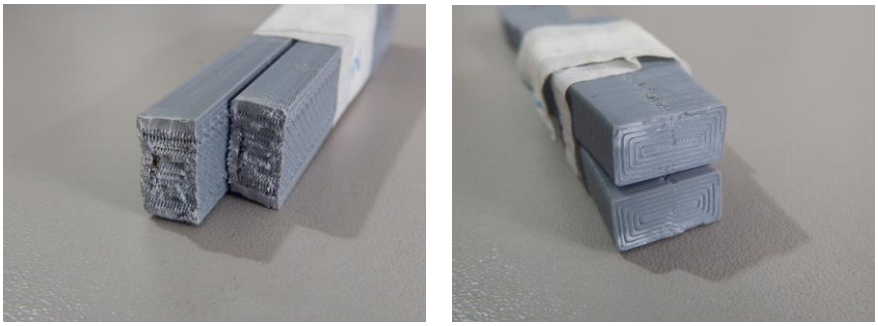

(a) (b)

Figure 9. (a) Specimen failure printed in ABS at 0 degree. (b) Specimen failure printed ABS at 90 degrees.

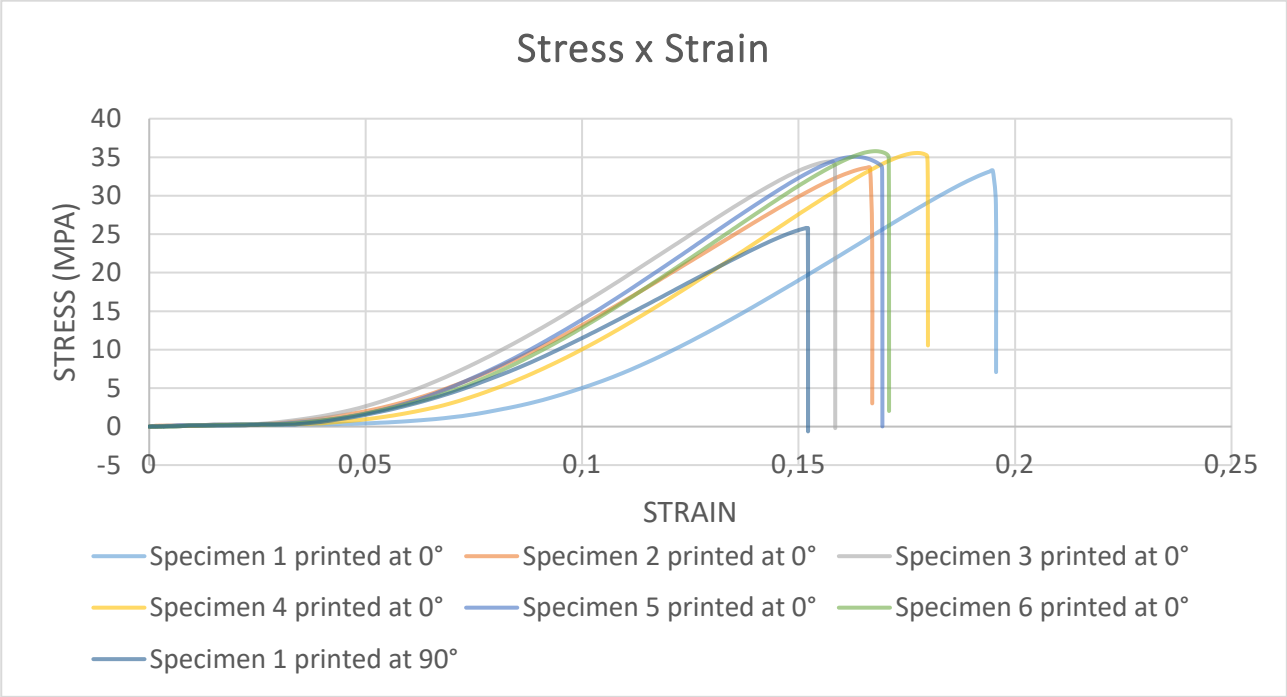

Figure 10. Stress-strain curves for specimens 3D-printed in ABS.

According to Table 5 and Figures 9 and 10:

i. All 3D-printed specimens presented brittle behavior at failure (see Fig. 9a);
ii. The average stress at break and the average maximum stress obtained are almost the same: 34,60 MPa and 34,57 MPa, respectively. These results are similar to the real values presented in Tab. 3 (33,9 MPa and 39.0 MPa, respectively);
iii. The average Young's modulus is 280.75 MPa, lower than the real value (1681.5 MPa – see Tab. 3). One reason for this difference maybe the test speed adopted (5mm/s) while Ultimaker technical data sheet ABS shows 1mm/s.

For the tensile test of the specimen 3D-printed at 90 degree (vertical direction), the maximum stress obtained was 25.79 MPa and, for the tensile stress at break, 25.33 MPa, with an elastic modulus of 249,03 MPa. Comparing these results with those presented in Tab. 5, it can be seen that the stress of 3D-printed specimen at 90 degree is about 74.5% of the 3D-printed specimen at 0 degrees. Yet, it was possible to verify that for the specimen 3D-printed at 90 degree, the failure occurred by detaching the layers of 3D printing (see Fig. 9b). However, for the specimens 3D-printed at 0 degrees, the failure was brittle. Kurauchi and Ohta, (1984) shows that 3D-printed components usually exhibit a brittle behavior.

4.2 Finite Element Analysis (FEA)

Table 6 presents the FEA results for each rotation imposed on the cutting chisel.

Table 6. FEA results.

Rotation (degree)	Displacement (mm)	Tresca Stress (MPa)
6	15,76	51,28
5	13,12	37,91
4	10,49	22,66
3	7,86	4,525
2	5,24	1,689
1	2,62	0,985
0	0	0,257

According to Table 6:

i. The greater the eccentricity of the chisel hammering, the greater the Tresca stress generated in the surgical guide;
ii. For rotations up to 4 degrees and displacements up to 10,49 mm, the Tresca stress in the guide was smaller than the tensile stress at break (33.9 MPa see Tab. 3), that is, the guide would withstand the surgical procedure without failure;
iii. For the maximum rotation angle considered (6 degrees), the Tresca stress obtained in the guide was 51.28 MPa, (see Fig 12), higher than the tensile stress at break (33.9 MPa see Tab. 3).

Figure 11 presents the Tresca stress distribution in the region of the guide cavity and the screw, considering a rotation of 4 degrees. It can be seen that the corner region of the cavity becomes a stress concentrator due to the more intense contact with the surface of the chisel.

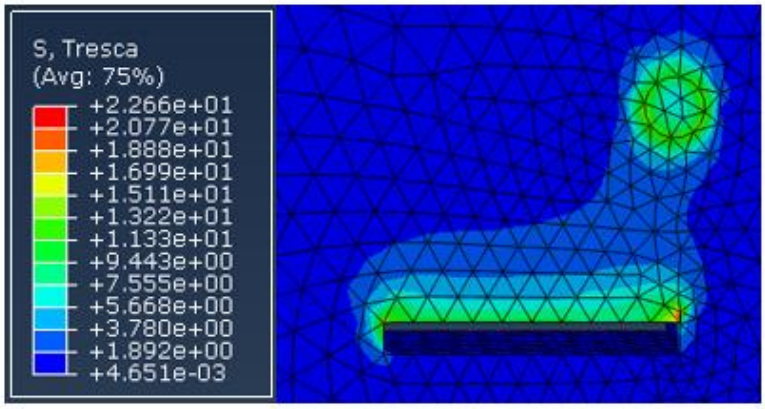

Figure 11. Distribution of Tresca stress in the guide, for a rotation of 4 degrees.

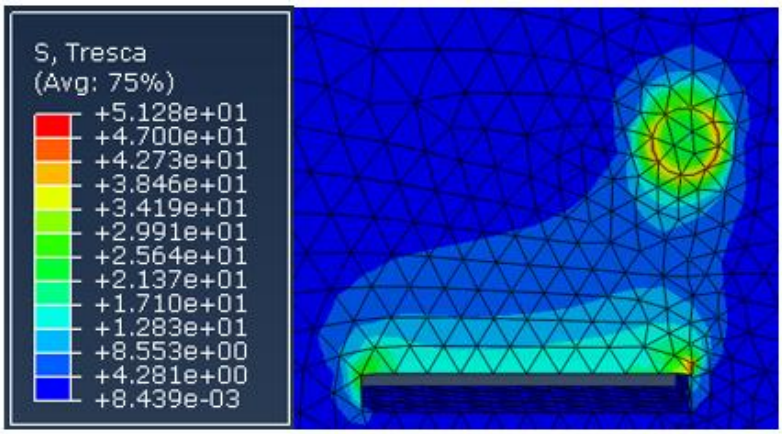

Figure 12. Distribution of Tresca stress in the guide, for a rotation of 6 degrees.

4. CONCLUSION

According to the results presented, the Meshmixer is a powerfull tool for the development of computational models, where the guide was created from the 3D model of the patient's hip bone with an anatomical shape and adaptable to the hip.

The tensile stress at break obtained by the tensile tests showed good correlation to the real value presented in Tab. 3. However, for the elastic modulus, there was a large difference in results that maybe due to test speed difference.

As expected, the higher the eccentricity which the surgeon hammers the chisel (and the higher the chisel rotation), the higher the Tresca stress distribution in the guide.

FEA analysis showed that the maximum rotation acceptable of the chisel by the guide is 4 degrees, corresponding to a maximum eccentricity of 10, 49 mm. For this rotation, the Tresca stress obtained remains under the tensile stress at break of the printed ABS (33.9 MPa – see Tab. 3).

For future work, it would be interesting to repeat the tensile tests with a speed of 1 mm/s in order to evaluate its influence in the elastic modulus results. Also, it would be interesting to perform FEA analysis of the computational model of the guide with the complex and irregular geometry generated by Meshmixer.

5. ACKNOWLEDGEMENTS

The authors are grateful for the support provided by the following agencies: FAPEMIG, Faculty of Engineering of the Federal University of Juiz de Fora and the Federal University of Juiz de Fora - UFJF.

6. REFERENCES

AKSteelCorporation (2007). "420 stainless steel data sheet". <http://www.aksteel.com/pdf/markets_products/stainless/martensitic/420_data_sheet.pdf>

Bitton, R., 2009. "The economic burden of osteoarthritis". In *American journal of managed care*. 01 Sep. 2009

Callister, William D, 2007. "Ciência e Engenharia dos Materiais, 7ª edição." (2007)

Cantrell, Jason, et al. 2017, "Experimental Characterization of the Mechanical Properties of 3D Printed ABS and Polycarbonate Parts." *Advancement of Optical Methods in Experimental Mechanics*, 08 Sep. 2016

Chegini, S., 2009. "The effects of impinge. Springer International Publishing, 2017. 89-105.ment and dysplasia on stress distributions in the hip joint during sitting and walking: a finite element analysis." In "*Journal of Orthopaedic Research"*. 27 Aug. 2008

Dalstra, M., et al., 1993 "Mechanical and textural properties of pelvic trabecular bone". In *Journal of biomechanics.* April–May, 1993

Ganz, R., Klaue, K., Vinh, T. S., and Mast, J. W.,1988. "A new periacetabular osteotomy for the treatment of hip dysplasias technique and preliminary results." In *"Clinical orthopaedics and related research",* Jul. 1988.

Hayasaki, Cláudio Luís, and Capello E. A., "Modelagem de estruturas ósseas e próteses através do Método dos Elementos Finitos*." Simpósio em Engenharia de Produção-Simpep".* 6 Nov 2006

İplikçioğlu, H., 2002 "Comparative evaluation of the effect of diameter, length and number of implants supporting three-unit fixed partial prostheses on stress distribution in the bone.*"Journal of dentistry"*. 1 Jan. 2002

Kurauchi, T, and T. Ohta, 1984. "Energy absorption in blends of polycarbonate with ABS and SAN". In *"Journal of materials science".* May 1984.

Ministério da Saúde, 2016. "Ministério da Saúde: Portal da saúde". 20 Oct. <portal.saude.gov.br>

Ultimaker, 2017. Technical data sheet ABS. < http://www.farnell.com/datasheets/2310520.pdf>

7. RESPONSIBILITY NOTICE

The authors are the only responsible for the printed material included in this paper.